Available online at www.sciencedirect.com
SCIENCE DIRECT®
Journal of Photochemistry and Photobiology A: Chemistry 162 (2004) 121–128
Journal of Photochemistry and Photobiology A:Chemistry
www.elsevier.com/locate/jphotochem

Formation efficiency of radical cations of stilbene and methoxy-substituted stilbenes during resonant two-photon ionization with a XeCl excimer laser

Michihiro Hara, Sachiko Tojo, Tetsuro Majima*

The Institute of Scientific and Industrial Research (SANKEN), Osaka University, Mihogaoka 8-1, Ibaraki, Osaka 567-0047, Japan

Received 13 May 2003; received in revised form 19 June 2003; accepted 5 July 2003

Abstract

Formation efficiency of radical cations of *trans*-stilbene and the methoxy-substituted stilbenes (**S** = ***1***–***6***) during the resonant two-photon ionization (RTPI) in acetonitrile has been studied by laser flash photolysis with a XeCl excimer laser (308 nm, 25 ns). The transient absorption spectra of **S** radical cations ($\mathbf{S}^{\bullet+}$) were observed with a peak around 450–540 nm. The formation quantum yield of $\mathbf{S}^{\bullet+}$ (Φ_{ion}) was 0.06–2.1%. No relation between Φ_{ion} and E^{ox} of **S** was observed, although Φ_{ion} increased with the increasing lifetime of **S** in the lowest excited singlet state (S_1). These results are coincident with a two-step two-photon excitation from the ground state (S_0) to S_1 and from S_1 to higher excited singlet state (S_n), and ionization from S_n. Considerably large Φ_{ion} was obtained for the RTPI of 3,5-dimethoxystilbene (**5**) with relatively high oxidation potential and a long S_1 lifetime among **S**. This is explained by the intermediacy of the internal charge-transfer excited state for the RTPI of **5** based on the fluorescence lifetime measurement, solvatochromic measurement, and the dipole moment calculation. The concentration of $\mathbf{S}^{\bullet+}$ increased with the increasing laser fluence (F). The log–log plot of [$\mathbf{S}^{\bullet+}$] versus F gave a linear line with a slope of approximately 2 for the RTPI of **1**–**4**, while approximately 1 for the RTPI of **5** and **6**. The slope of 2 indicates clearly two-photon excitation during the RTPI. The slope of 1 is explained by the photostationary state among S_0, S_1, and S_n states attained during the laser pulse, particularly for the RTPI of **S** with a long S_1 lifetime.

Keywords: Radical cation; Stilbene; Resonant two-photon ionization; XeCl excimer laser photolysis; Substituent effect; Lifetime of the singlet excited state

1. Introduction

The radical cations of molecules ($\mathbf{M}^{\bullet+}$) can be generated from one-electron oxidation such as electrochemical reaction, chemical oxidation using one-electron oxidants, photo-induced electron transfer, two-photon ionization, radiation chemical reaction, and so on [1–5]. Kinetic studies of $\mathbf{M}^{\bullet+}$ after the formation of $\mathbf{M}^{\bullet+}$ at a sufficiently high concentration up to 10^{-5} M are usually performed with laser flash photolysis and pulse radiolysis [6–9]. We have been investigating the formation and reactivity of radical cations of stilbene and substituted stilbenes during photo-induced electron transfer reaction [6] and during pulse radiolysis [7–9]. We report here the formation of radical cations of a series of stilbene and methoxy-substituted stilbenes during the resonant two-photon ionization (RTPI) with a XeCl excimer laser as a convenient intense pulsed laser.

The RTPI of **M** occurs to give $\mathbf{M}^{\bullet+}$ and an electron with irradiation at a high laser fluence (F in J cm^{-2} per pulse) using an intense short-pulsed laser with a wavelength tuned to the absorption of the molecules [10–22]. The RTPI has been observed during the LFP of many aromatic molecules such as aromatic olefins [10,22], arenes [11–20,23], and aromatic amines [21] because of their relatively low oxidation potentials and strong absorption in the UV-Vis region. A first excitation of **M** generates **M** in the S_1 state ($^1\mathbf{M}^*$), and a second excitation of $^1\mathbf{M}^*$ gives **M** in a higher excited singlet state ($^1\mathbf{M}^{**}$). When the energy of $^1\mathbf{M}^{**}$ is higher than the ionization energy of **M**, electron detachment of $^1\mathbf{M}^{**}$ occurs to give $\mathbf{M}^{\bullet+}$ and an electron, competitively with the internal conversion. For example, pyrene (Py) and substituted Py in the S_1 state have a sufficiently long S_1 lifetime $\tau(S_1)$ such as a few tens of nanoseconds, and their RTPI is known during their laser photolyses using an intense short-pulsed laser [21,24]. In addition to the RTPI of **M** with a relatively long $\tau(S_1)$ such as diarylethylene and Py, the RTPI of stilbene with short $\tau(S_1)$ has been recently studied in several solvents by ps pump-probe CARS [1,25–27] and in acetonitrile

* Corresponding author. Tel.: +81-6-6879-8495; fax: +81-6-6879-8499.
E-mail address: majima@sanken.osaka-u.ac.jp (T. Majima).

1010-6030/$ – see front matter © 2004 Elsevier B.V. All rights reserved.
doi:10.1016/S1010-6030(03)00321-6

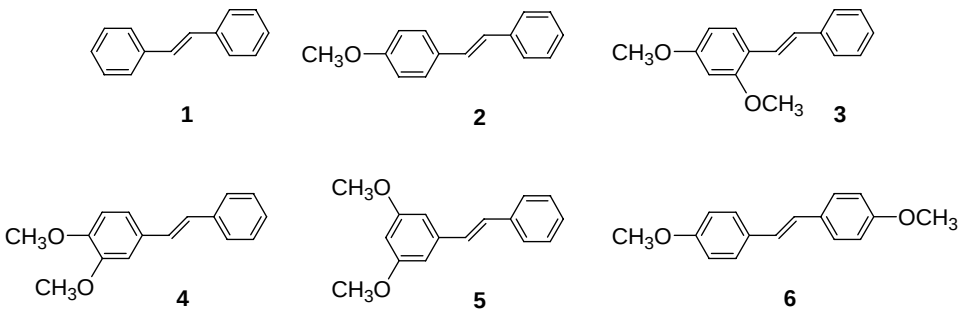

Scheme 1.

by ps time-resolved Raman spectral measurement [28]. The yield of the stilbene radical cation has been found to depend on the solvent, and the formation rate of the stilbene radical cation from stilbene in the S_1 state has been determined to be on a 40–60 ps time scale in acetonitrile [28].

In order to use the RTPI as a method of generating stilbene radical cations in high yields for the kinetic measurement, we have studied the RTPI of a series of stilbenes (**S** = ***1***–***6***, *trans*-stilbene **1** and *trans*-4-methoxystilbene **2**, and *trans*-2,4-, -3,4-, -3,5-, and -4,4′-dimethoxystilbenes **3**, **4**, **5**, and **6**, respectively, Scheme 1) in acetonitrile with irradiation using a XeCl laser (260 mJ, 25 ns FWHM) at the 308 nm wavelength and a high *F*. Particular interest is focused on elucidation of important factors for the formation efficiency of **S** radical cations ($\mathbf{S}^{\bullet+}$).

2. Experimental section

2.1. Materials

1 (>99.5%) was purchased from Tokyo Kasei and purified by recrystallization from ethanol before use. The substituted stilbenes (**2**–**6**) were synthesized by the Wittig reaction of the corresponding substituted benzaldehyde and benzyltriphenylphosphonium chloride with sodium ethoxide in absolute ethanol at room temperature according to literature procedures [29–34] and recrystallized from ethanol before use. 4-Methoxystilbene (**2**), mp: 137–138 °C (136–137 °C [32]); 2,4-dimethostilbene (**3**), mp: 62–63 °C (62–63 °C [29]); 3,4-dimethoxystilbene (**4**), mp: 107–108 °C (111 °C [30]); 3,5-dimethoxystilbene (**5**), mp: 47–48 °C (56 °C [31]); 4,4′-dimethoxystilbene (**6**), mp: 214–215 °C (214.5–215 °C [31]). Acetonitrile, dimethylsulfoxide (DMF), and tetrahydrofuran (THF) (Kishida Kagaku; spectroscopic grade), methanol (MeOH), butylalcohol and cyclohexane (Nacalai Tesque; spectroscopic grade), *iso*-propylalcohol (2-PrOH), 1,2-dichloroethane (DCE), diethylether (DEE), chloroform, *iso*-octane, and *n*-hexane (Wako spectroscopic grade) was used without further purification. 9,10-Dicyanthracene (DCA) was purchased from Aldrich and purified by recrystallization from benzene before use. Biphenyl (Bp) was purchased from Wako and purified by recrystallization from ethanol before use.

2.2. Absorption and fluorescence spectral measurements

UV Spectra were measured in acetonitrile by a Shimadzu UV-3100PC UV-Vis spectrometer with a transparent rectangular cell made from quartz (1.0 cm × 1.0 cm × 4.0 cm, path length of 1.0 cm). Fluorescence spectra were measured by a JASCO FP-500 (A) spectrofluorimeter at 25 °C. The light

Table 1
Oxidation potentials and absorption and fluorescence spectral data of **1** and substituted stilbenes (**2**–**6**) in Ar-saturated acetonitrile

S	$(E^{ox})^a$ (V)	Absorption		Fluorescence				Stokes shift (nm)
		λ_{max} (nm)	ε_{max} ($M^{-1}\,cm^{-1}$)	λ_{max} (nm)	$(\Phi_f)^b$	$(\tau_f)^c$ (ps)	$\tau(S_1)^d$ (ns)	
1	1.27	307	3.3×10^4	349	0.016	39	nd	42
2	0.89	317	2.5×10^4	373	0.003	7	nd	56
3	0.73	331	2.2×10^4	391	0.001	5	nd	60
4	0.79	325	2.9×10^4	384	0.008	19	nd	59
5	1.22	308	2.9×10^4	392	0.023	76	4	84
6	0.75	326	3.0×10^4	373	0.080	30	0.35[e]	47

nd: not determined because of $\tau(S_1)$ shorter than 1 ns.
[a] Peak voltage for the irreversible oxidation vs. Ag/Ag.
[b] Fluorescence quantum yield.
[c] Lifetime of $^1\mathbf{S}^*$ calculated from the Sticker-Barge equation (see text).
[d] Measured by ns time-resolved SPC.
[e] According to [37].

source for the excitation was a 150 W Xe lamp (Toshiba). A photomultiplier (Hamamatsu R928) was used for the detector.

The absorption peak was observed around 307–331 nm, while the fluorescence peak was around 349–392 nm depending on **S**. The Stokes shifts were 42–60 nm for **S** except for **5**, while it was 84 nm for **5**. The fluorescence quantum yield of **S** (Φ_f) was determined from the integrations of the fluorescence using an external standard of **1** in acetonitrile ($\Phi_{f}\mathbf{1} = 0.016$) [35] and molar absorption coefficients of **1** and **S**. The fluorescence lifetimes (τ_f) were calculated from the molecular absorption coefficient at the peak and band width of the peak according to the Sticker-Barge equation [36] as shown in Table 1.

3. Lifetime measurement with single-photon counting

$\tau(S_1)$ was measured by ns time-resolved single-photon counting (SPC) (Horiba NAES-1100) using a quartz rectangular cell (1.0 cm × 1.0 cm × 4.0 cm, path length of 1.0 cm). Here, we use $\tau(S_1)$ for fluorescence lifetimes measured by SPC, and τ_f for fluorescence lifetimes based on the Sticker-Barge equation [36]. The fluorescence and scatter signals were detected with NFL 111 ns lamp and SSU-111 photomultiplier. The fluorescence decays were analyzed by the least-square iterative deconvolution method. The absorbance of the degassed specimens was less than 0.1 in acetonitrile. The value of $\tau(S_1) = 4$ ns measured for **5** was 10 times longer than the calculated $\tau_f = 76$ ps (Table 1). The $\tau(S_1)$ values of other **S** were shorter than 1 ns and out of the detection limit. The $\tau(S_1) = 0.35$ ns for **6** in the S_1 state has been measured by the ns time-resolved single-photon counting [37].

3.1. Solvatochromic measurement

Because the largest Stokes (84 nm) shift and longest lifetime (4 ns) were observed only in **5**, the internal charge-transfer (CT) character is suggested for the character of **5** in the S_1 state. Solvatochromic measurement was thus carried out. The presence of the CT excited state has been assumed based on the solvatochromic effects of *p*-dimethylaminobenzonitrile [38,39] and *trans*-4-dimethylamino-4′-cyanostilbene [40] on their absorption and fluorescence spectra. Absorption and fluorescence spectra of **5** were measured in various solvents such as acetonitrile, dimethylsulfoxide, and tetrahydrofuran, methanol, butylalcohol, and cyclohexane, *iso*-propylalcohol, 1,2-dichloroethane, diethylether, chloroform, *iso*-octane, and *n*-hexane. The solvatochromic shifts of the maxima peaks (ν_{abs} and ν_f) of the absorption and fluorescence spectra of **5** are indicated as the straight lines of plots of ν_{abs} and ν_f versus the solvent polarity function (Δp) [40] with the slopes of *m*(abs) and *m*(f), respectively, as shown in Fig. 1. Dipole moments of the S_1 state and CT excited state of **S** were calculated from the

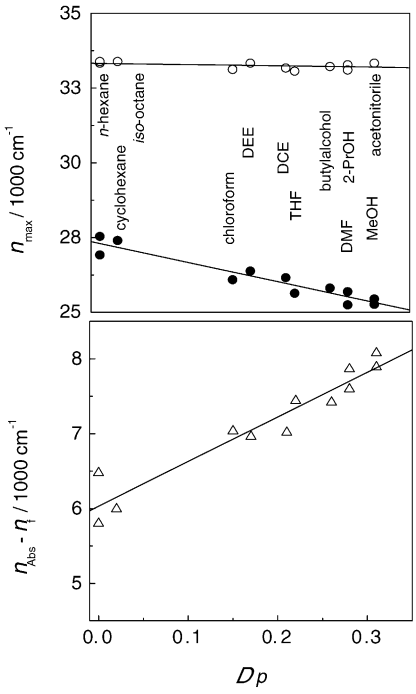

Fig. 1. Plots of ν_{max} of absorption (○), fluorescence (●), and Stokes shift ($\nu_{abs} - \nu_f$, △) vs. the solvent polarity function (Δp) for **5**.

solvatochromic slopes of *m*(abs) and *m*(f) to be $\mu_{S_1} = 3.1$ and $\mu_{CT} = 9.1$ D, respectively, based on $\mu_g = 2.3$ D using the MOPAC AM1 method. In contrast, little change was observed for the peaks, shapes, absorbance, and intensities depending on the solvent in the absorption and fluorescence spectra of **1** and **2**.

3.2. Nanosecond laser flash photolysis

Nanosecond laser flash photolysis experiments were carried out using 308 nm flash from a XeCl excimer laser (Lambda Physik Compex 102; pulse width of 25 ns FWHM, laser intensity of 50–200 mJ per pulse, and *F* of 128–512 mJ cm^{-2} per pulse) and the third harmonic oscillation (355 nm) of a Nd^{3+}:YAG laser (Quantel Brilliant Q-switch laser; pulse width of 5 ns FWHM) as an excitation source. The monitor light source was obtained from a 450 W Xe lamp (Osram XBO-450) synchronized with the laser flash. The irradiation volume of the laser beam was identical with that of the monitor light source. The intensity of the monitor light source was detected using a photomultiplier (Hamamatsu R928). The electric signal from the photomultiplier was digitalized by an oscilloscope and transmitted to a personal computer with the interface RS 232C. The signals were accumulated. Transient absorption spectra were measured by a multichannel analyzer with an image intensifier having a 30 ns gate width and transmitted to a personal computer with the interface RS 232C. The spectra were accumulated (Unisoku 1-02). The samples were prepared in degassed or saturated with Ar for

15 min, using a transparent rectangular cell made of quartz (1.0 cm × 1.0 cm × 4.0 cm, light-path length of 1.0 cm) at room temperature. The concentration of S was chosen to have an absorbance of 1.0 at 308 nm of the excitation laser wavelength.

3.3. Oxidation potential measurement

Oxidation potentials (E^{ox}) were measured in acetonitrile by cyclic voltammetry (BAS Model CV-50 W voltammograph) with platinum working and auxiliary electrodes and a Ag/Ag^+ reference electrode at a scan rate of 50 mV s^{-1}. Ferrocene ($E^{ox} = 0.76$ V) was used as a standard external reference. Measurements were performed in dry acetonitrile containing 1.0×10^{-3} M of **S** and 0.1 M tetraethylammonium tetrafluoroborate electrolyte. Because the cyclic voltagrams gave irreversible oxidation peaks, the peak potentials were taken for E^{ox} (Table 1). E^{ox} values of **S** were 0.89–1.42 V.

All experiments of spectral measurements, transient absorption measurements, and oxidation potential measurements were carried out at room temperature.

4. Results

4.1. Transient absorption measurement of $S^{\bullet+}$ during the RTPI of S

A transient absorption spectrum with a maximum peak at $\lambda_{max} = 472$ nm was observed during the 308 nm laser flash photolysis of **1** in acetonitrile (3.8×10^{-5} M) at $F = 512$ mJ cm^{-2} per pulse (Fig. 1). The transient absorption decreased with lower F. The transient absorption spectrum was reasonably assigned to the **1** radical cation ($\mathbf{1}^{\bullet+}$) according to the previous report [41]. Concentrations of the sample solution were set at the absorbance of 1.0 for the sample solution with a 1 cm optical length at the excitation wavelength (308 nm). From the relationship between the ionization potential of **1** (7.8 eV) and the photon energy of a XeCl laser (4.0 eV), **1** is ionized by two-photon excitation at 308 nm. Similarly, transient absorption spectra of $\mathbf{S}^{\bullet+}$ with peaks around 450–540 nm were observed in the region of 400–600 nm, although the peaks were much broader, two peaks were observed for $\mathbf{2}^{\bullet+}$ and $\mathbf{5}^{\bullet+}$, and the peaks of $\mathbf{5}^{\bullet+}$ and $\mathbf{6}^{\bullet+}$ shifted to the longer wavelength. Because a 308 nm photon energy is not sufficient for the ionization of **S**, $\mathbf{S}^{\bullet+}$ is generated during the RTPI of other **S** types at 308 nm in acetonitrile.

An electron is generated together with $\mathbf{S}^{\bullet+}$, and the electron then reacts with acetonitrile to give an acetonitrile radical anion and a dimer radical anion which have a weak absorption in the range of 400–600 nm [42]. Even a solvated electron reacts partly with **1** at a rate constant of $(2–5) \times 10^{10}$ M^{-1} s^{-1} [43], The **1** radical anion cannot be generated on a time scale of 100 ns at a concentration of 10^{-5} M of **1**. In fact, no transient absorption of the **1** radical anion with a peak at 530 nm was observed at 100 ns after the laser flash during the RTPI of **1** (3.8×10^{-5} M) in acetonitrile as shown in Fig. 2.

4.2. Formation quantum yield of $S^{\bullet+}$ (Φ_{ion}) of the RTPI

The molar absorption coefficients (ε) of $\mathbf{S}^{\bullet+}$ at a wavelength of the absorption is necessary to determine the concentration of $\mathbf{S}^{\bullet+}$. The formation of $\mathbf{1}^{\bullet+}$ and $\mathbf{6}^{\bullet+}$ has been observed during the pulse radiolyses in DCE at room temperature [6–8], γ-radiolysis in butyl chloride solution at 77 K [9], and photo-induced electron transfer between DCA in the singlet excited state (^{1}DCA*) and Bp in acetonitrile at room temperature [44,45]. The molar absorption coefficients (ε) of all $\mathbf{S}^{\bullet+}$ determined from the photo-induced electron transfer were used in the present study because acetonitrile was the solvent in both experiments.

The transient absorption spectrum of the Bp radical cation ($Bp^{\bullet+}$) was observed at the end of the laser flash during 355 nm 5 ns flash photolysis of a mixture of DCA (0.1 mM), Bp (100 mM), and **6** (1 mM) in acetonitrile. The $Bp^{\bullet+}$ absorption decayed together with the formation of a new peak at 530 nm assigned to $\mathbf{6}^{\bullet+}$. These are responsible for electron transfer from Bp to ^{1}DCA* to form $Bp^{\bullet+}$, and a DCA radical anion ($DCA^{\bullet-}$) and hole transfer from $Bp^{\bullet+}$ to **5**. From the maximum $\Delta O.D._{670} = 0.026$ of $Bp^{\bullet+}$, $[Bp^{\bullet+}]$ was calculated to be 1.8×10^{-6} M using $\varepsilon_{670} = 1.45 \times 10^4$ M^{-1} cm^{-1} [46]. $[Bp^{\bullet+}] = [\mathbf{6}^{\bullet+}]$ is assumed; therefore, ε at 540 nm ($\varepsilon_{540} = 4.1 \times 10^4$ M^{-1} cm^{-1}) was calculated for $\mathbf{6}^{\bullet+}$. Similarly, ε values for the absorption of $\mathbf{S}^{\bullet+}$ at the wavelength monitored were calculated: $\varepsilon_{480} = 4.7 \times 10^4$ for $\mathbf{1}^{\bullet+}$, $\varepsilon_{485} = 6.1 \times 10^4$ for $\mathbf{2}^{\bullet+}$, $\varepsilon_{480} = 3.3 \times 10^4$ for $\mathbf{3}^{\bullet+}$, $\varepsilon_{480} = 3.4 \times 10^4$ for $\mathbf{4}^{\bullet+}$, and $\varepsilon_{480} = 2.5 \times 10^4$ M^{-1} cm^{-1} for $\mathbf{5}^{\bullet+}$.

From $[\mathbf{1}^{\bullet+}] = 2.0 \times 10^{-6}$ M, the quantum yield was calculated to be $\Phi_{ion} = 2.0 \times 10^{-3}$ for the RTPI of $\mathbf{1}^{\bullet+}$ at $F = 512$ mJ cm^{-2} per pulse. Similarly, Φ_{ion} values for $\mathbf{S}^{\bullet+}$ were obtained as shown in Table 2.

4.3. Relationship between Φ_{ion} and F

The Φ_{ion} calculated from the concentration of $\mathbf{S}^{\bullet+}$ increased with the increasing F. The log–log plot of $[\mathbf{1}^{\bullet+}]$

Table 2
Quantum yield of the RTPI (Φ_{ion}) and slope of linear plots of $\log[\mathbf{S}^{\bullet+}]$ vs. $\log F$

S	$\mathbf{S} \rightarrow \mathbf{S}^{\bullet+} + e^-$	
	$(\Phi_{ion})^a \times 10^{-3}$	Slope
1	2.0	1.9
2	0.6	2.0
3	1.4	1.7
4	6.0	1.8
5	20.7	0.8
6	12.6	1.2

[a] At $F = 512$ mJ cm^{-2} per pulse in acetonitrile.

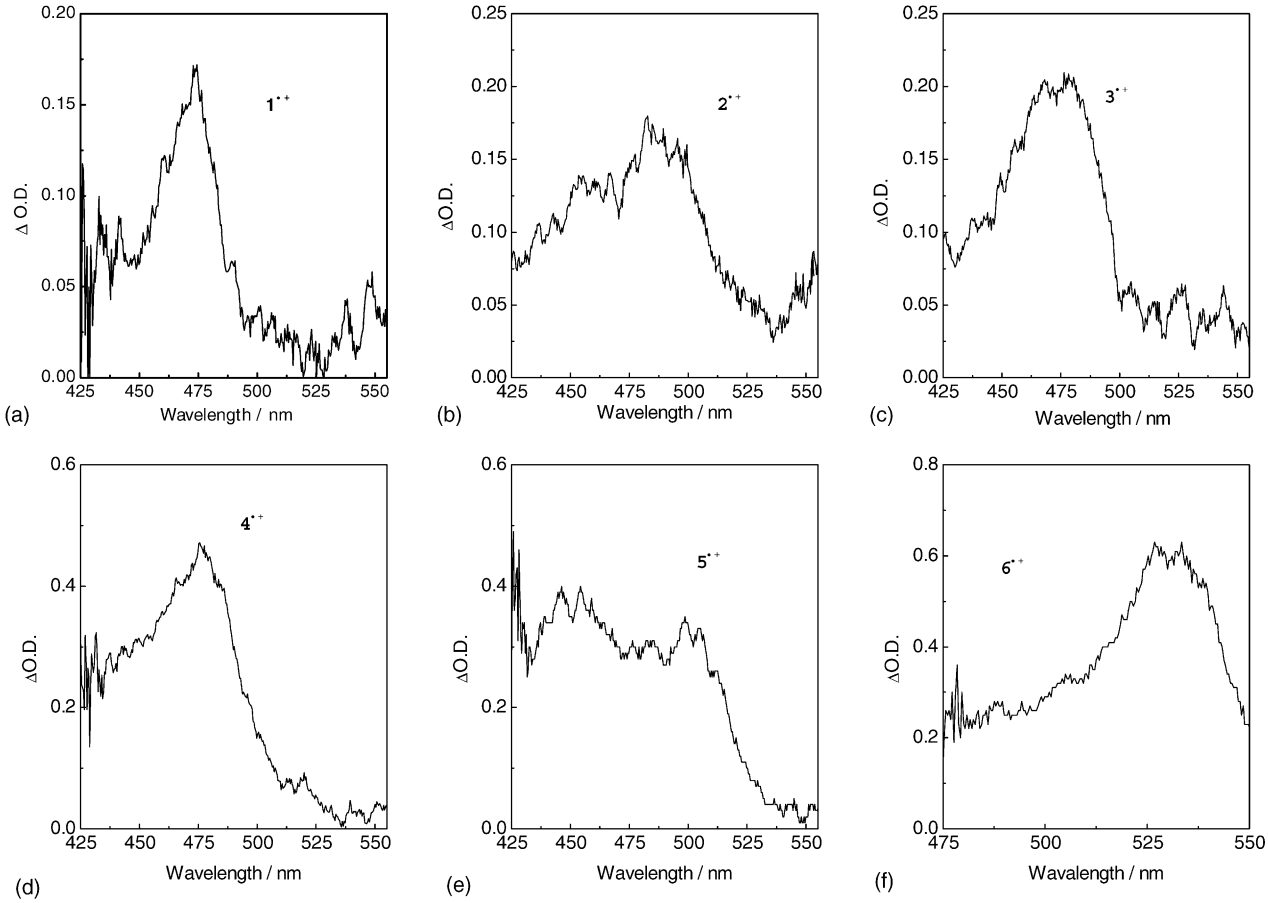

Fig. 2. Transient absorption spectra assigned to $\mathbf{S}^{\bullet+}$ observed at the end of a laser flash with $I = 200\,\text{mJ}$ per pulse and $F = 512\,\text{mJ cm}^{-2}$ per pulse (large ΔO.D.), and $I = 100\,\text{mJ}$ per pulse and $F = 128\,\text{mJ cm}^{-2}$ per pulse (small ΔO.D.) during the RTPI of **S** at 308 nm in acetonitrile. Concentrations of **1** (a), **2** (b), **3** (c), **4** (d), **5** (e), and **6** (f) were 3.8×10^{-5}, 4.0×10^{-5}, 6.3×10^{-5}, 4.7×10^{-5}, 3.7×10^{-5}, and 2.7×10^{-5} M, respectively.

versus F showed a linear relationship with a slope of 2, which indicates that the Φ_{ion} of $\mathbf{1}^{\bullet+}$ is proportional to F^2 (Fig. 3). A slope of approximately 2 was also obtained for the RTPI of **2**–**4** as shown in Table 2, indicating two-photon excitation during the RTPI. On the other hand, the slopes of 0.8 and 1.2 were obtained for the linear log–log plots of [$\mathbf{5}^{\bullet+}$] and [$\mathbf{6}^{\bullet+}$], respectively, versus F (Fig. 3). The slopes of plots of log[$\mathbf{S}^{\bullet+}$] versus log F were summarized in Table 2. The slope means the photon number required to produce $\mathbf{S}^{\bullet+}$ in the RTPI. The slope of approximately 1 for the RTPI of **5** and **6** would suggest one-photon process for the formation of $\mathbf{5}^{\bullet+}$ and $\mathbf{6}^{\bullet+}$, although the RTPI of **5** and **6** occurs with two-photon excitation. A mechanism of the RTPI of **5** and **6** is suggested to be different from that of **1**–**4**.

4.4. Relationships between Φ_{ion} and E^{ox} or τ_{f}

The effects of the physical properties of **S** on the Φ_{ion} were examined. No relation between the Φ_{ion} (0.06–0.29%) and E^{ox} of **S** was observed (Fig. 4). On the other hand, Φ_{ion} increased with the increasing τ_{f} of $^1\mathbf{S}^*$ (Fig. 5).

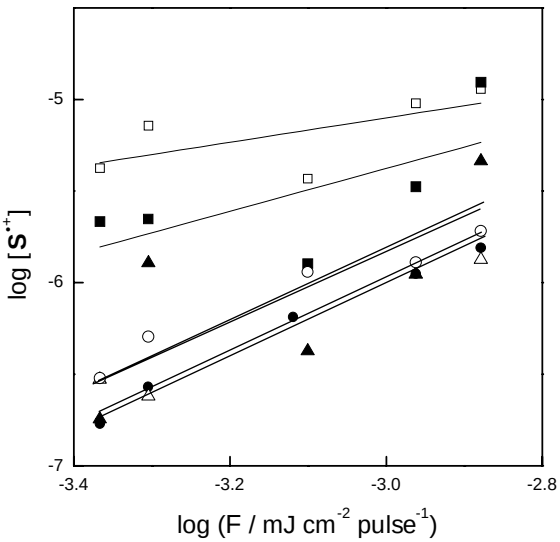

Fig. 3. Log–log plots of [$\mathbf{S}^{\bullet+}$] (in M) vs. laser fluence (F in mJ cm^{-2} per pulse). [$\mathbf{S}^{\bullet+}$] values were calculated from ΔO.D. at 480, 485, 480, 480, 480, and 540 nm of $\mathbf{1}^{\bullet+}$ (○), $\mathbf{2}^{\bullet+}$ (●), $\mathbf{3}^{\bullet+}$ (△), $\mathbf{4}^{\bullet+}$ (▲), $\mathbf{5}^{\bullet+}$ (□), and $\mathbf{6}^{\bullet+}$ (■), respectively.

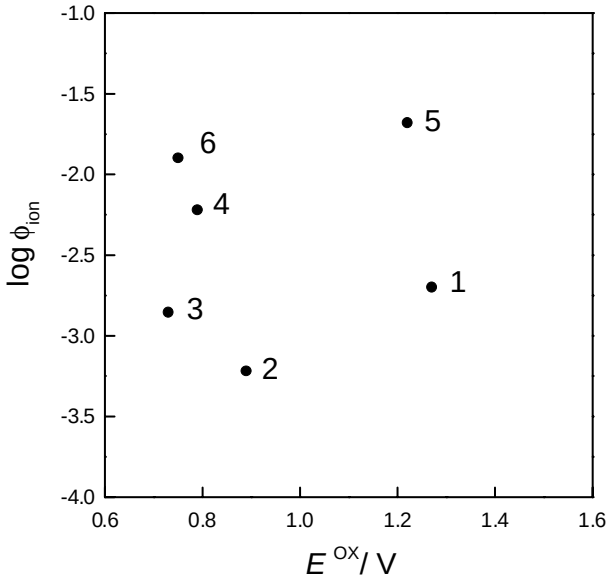

Fig. 4. Plot of $\log \Phi_{ion}$ vs. E^{ox}.

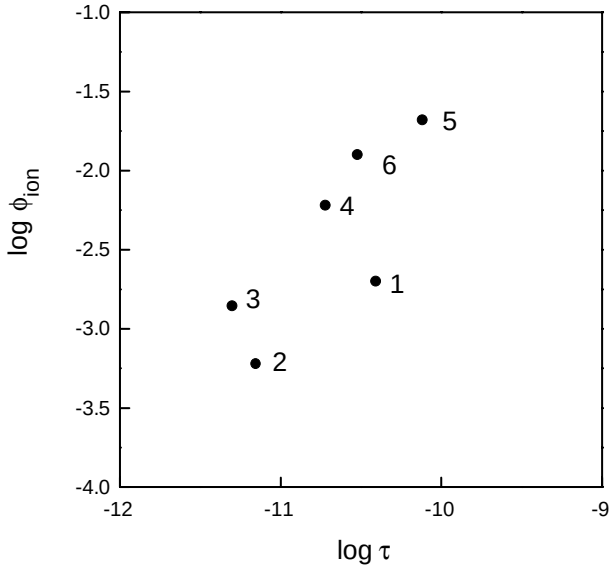

Fig. 5. Plot of $\log \Phi_{ion}$ vs. $\log \tau_f$.

5. Discussion

5.1. Mechanism of the RTPI of 1–4

It is found that $\mathbf{S}^{\bullet+}$ ($\mathbf{1}^{\bullet+}$–$\mathbf{4}^{\bullet+}$) is generated during the RTPI in which **S** is excited to the S_1 state ($^1\mathbf{S}^*$) with the first-photon excitation at 308 nm, and $^1\mathbf{S}^*$ is then excited to the S_n state with the second-photon excitation at 308 nm during the single laser pulse irradiation (25 ns). The concentration of $\mathbf{S}^{\bullet+}$ was proportional to F^2 for $\mathbf{1}^{\bullet+}$–$\mathbf{4}^{\bullet+}$ (Table 2). This relation is usually obtained for the RTPI because two-photon absorption is necessary for ionization

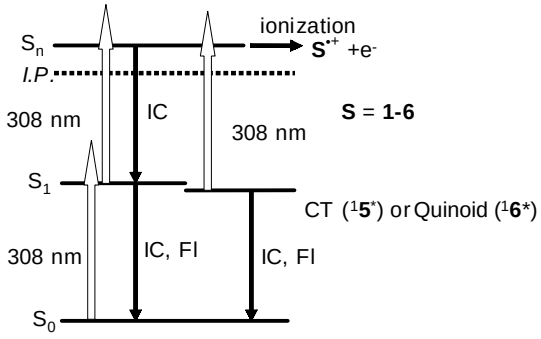

Scheme 2.

of **S** to give $\mathbf{S}^{\bullet+}$. Therefore, stepwise excitation of **S** involving first excitation to the S_1 state and second excitation to the S_n state is followed by electron detachment from the S_n state to give $\mathbf{S}^{\bullet+}$ during the RTPI of **1**–**4** as shown in Scheme 2 where IP, IC, and Fl are the ionization potential, internal conversion, and fluorescence, respectively.

Because the peaks and shapes of the absorption and emission spectra of **1**–**4** in various solvents were similar, the S_0–S_1 absorption is assigned to the $\pi\pi^*$ transition with a similar S_0–S_1 energy gap. On the other hand, E^{ox} changed from 0.73 to 1.27 V and τ_f (5–39 ps) changed 7–8 times. No relation between Φ_{ion} (0.06–2.1%) and E^{ox} of **1**–**4** was observed (Fig. 4), although Φ_{ion} increased with increasing τ_f (Fig. 5).

According to the mechanism of the RTPI of **1**–**4** (Scheme 2), Φ_{ion} is expected to increase with lower E^{ox}, longer τ_f, and larger transition probabilities of the S_0–S_1 and S_1–S_n excitations. The relation of larger Φ_{ion} with lower E^{ox} has been generally found for the RTPI of various molecules. However, E^{ox} was not an important factor in the RTPI of a series of molecules such as **S** (**1**–**4**). Because the two-photon energy of 308 nm light is 8.0 eV, which is higher than the ionization energies of **S**, the difference in E^{ox} does not influence the Φ_{ion}. On the other hand, the effect of τ_f appeared clearly on Φ_{ion}. The concentration of **1**–**4** was chosen to have an absorbance of 1.0 at 308 nm of the excitation laser wavelength; thus, the transition probability of the S_0–S_1 excitation does not appear in Φ_{ion}. The transition probability of the S_1–S_n excitation is definitely an important factor for Φ_{ion}, although it is not known. Consequently, it is found that **S** should be designed to have a longer τ_f of $^1\mathbf{S}^*$ in order to obtain a high Φ_{ion} during the RTPI.

5.2. Mechanism of the RTPI of 5 and 6

The relation of $[\mathbf{S}^{\bullet+}]$ proportional to F (slope = 1) was obtained for the RTPI of **5** and **6**. **5** has the second highest E^{ox} of 1.22 V, the longest τ_f of 76 ps, and the largest $\Phi_{ion} = 2.07 \times 10^{-2}$ among **S**. **6** has the second lowest E^{ox} of 0.75 V, the second longest τ_f of 30 ps, and the second largest $\Phi_{ion} = 1.26 \times 10^{-2}$ among **S**. Because concentrations of the sample solutions were set at the absorbance of 1.0 at the 308 nm

excitation wavelength, the excitation from the S_0 to S_1 state proceeds similarly for all **S**. The relation between Φ_{ion} and F is thus explained by a photostationary state with constant concentrations of **5** and **6** in the S_1 and S_n states which are attained within the laser flash duration. It should be noted again that the Φ_{ion} depends not on E^{ox} but on τ_f (Figs. 4 and 5).

According to dipole moments calculated for **5** in the S_0 and S_1 states, a CT excited state with a long $\tau(S_1) = 4$ ns is assumed for **5** in the S_1 state, which is responsible for the efficient second excitation to **5** in the S_n state to give $\mathbf{5}^{\bullet+}$ in a large Φ_{ion} (Scheme 2). Because **6** has two methoxyl groups substituted symmetrically to the two benzene rings, such CT excited state cannot be expected for **6** in the S_1 state. However, the second excitation occurs very efficiently from **6** in the S_1 state to the S_n state at the 308 nm laser wavelength. The lifetime of 0.35 ns for **6** in the S_1 state has been measured by the time-resolved single-photon counting [37], although such long lifetimes for other **S** in the S_1 state were not observed. **2**–**4** have one or two methoxyl substituents on one benzene ring, while **6** has two 4-methoxyl substituents symmetrically on two benzene rings. Therefore, it is suggested that **6** in the S_1 state is stabilized and has the longer lifetime of 0.35 ns because of the quinoid-type electronic structure involving not only π-electrons but also n-electrons of oxygen atoms of two methoxyl substituents, which contributes much less in **2**–**4** in the S_1 state.

The slope of 1 can be obtained for the RTPI of **M** with relatively long $\tau(S_1)$ of $^1\mathbf{M}^*$. It should be generally considered that the RTPI of **M** generates $\mathbf{M}^{\bullet+}$ effectively via the CT excited state even if **M** has a relatively high E^{ox}. It is suggested that the CT excited state has probably larger absorption cross-section for the second excitation to the S_n state at the laser wavelength. The intermediacy of the CT excited state is also assumed for non-linear light absorption enhanced by the CT excited state [47,48]. Consequently, it is found that the RTPI of **S** reflects the properties of the intermediate in the S_1 state, and the slope of 2 is not essential for the RTPI.

6. Conclusions

$\mathbf{S}^{\bullet+}$ was generated from the RTPI of **S** in acetonitrile with irradiation of a XeCl laser pulse with high F. Φ_{ion} was proportional to F^2 for the RTPI of **1**–**4**, although Φ_{ion} was and proportional to F for the RTPI of **5** and **6**. No relation between Φ_{ion} (0.06–0.29%) and E^{ox} of **S** was observed, although Φ_{ion} increased with the increasing τ_f. Based on these results, together with the relationship between the ionization energy of **S** and the photon energy of a XeCl laser, the RTPI proceeds via a two-step two-photon excitation through $^1\mathbf{S}^*$ and ionization from the S_n state. The intermediacy of the internal CT excited state for the RTPI of **5** was suggested based on the fluorescence lifetime measurement, solvatochromic measurement, and the dipole moment calculation. The RTPI of **S** reflects the properties of the intermediate in the S_1 state. Although the slopes of the log–log plots of $[\mathbf{S}^{\bullet+}]$ versus F has been frequently discussed as a proof of the RTPI, it is found that the slope of approximately 2 is not essential for the RTPI. The slope of approximately 1 observed for the RTPI of **5** and **6** is explained by the photostationary state among S_0, S_1, and S_n states attained during the laser pulse in the RTPI. It is suggested that **S** should be designed to have a longer τ_f of $^1\mathbf{S}^*$ such as the CT excited state in order to obtain a high yield of $\mathbf{S}^{\bullet+}$ for the kinetic measurement of $\mathbf{S}^{\bullet+}$ during the RTPI.

Acknowledgements

This work was partly supported by a Grant-in-Aid for Scientific Research from Ministry of Education, Culture, Sports, Science and Technology of Japan.

References

[1] M.A. Fox, Chem. Rev. 79 (1979) 253.
[2] M. Julliard, M. Chanon, Chem. Rev. 83 (1983) 425.
[3] G.J. Kavarnos, N.J. Turro, Chem. Rev. 86 (1986) 401.
[4] F.D. Lewis, R.L. Letsinger, M.R. Wasielewski, Acc. Chem. Res. 34 (2001) 159.
[5] E. Baciocchi, M. Bietti, M. Salamone, S. Steenken, J. Org. Chem. 67 (2002) 2266.
[6] T. Majima, S. Tojo, A. Ishida, S. Takamuku, J. Org. Chem. 61 (1996) 7793.
[7] A. Ishida, M. Fukui, H. Ogawa, S. Tojo, T. Majima, S. Takamuku, J. Phys. Chem. 99 (1995) 10808.
[8] T. Majima, S. Tojo, A. Ishida, S. Takamuku, J. Phys. Chem. 100 (1996) 13615.
[9] S. Tojo, K. Morishima, A. Ishida, T. Majima, S. Takamuku, Bull. Chem. Soc. Jpn. 68 (1995) 958.
[10] J.L. Faria, S. Steenken, J. Phys. Chem. 97 (1993) 1924.
[11] V.A. Kuzmin, A. Dourandin, V. Shafirovich, N.E. Geacintov, Phys. Chem. Chem. Phys. 2 (2000) 1531.
[12] K.H. Schmidt, M.C. Sauer, Y.L. Lu, A.D. Liu, J. Phys. Chem. 94 (1990) 244.
[13] V. Shafirovich, A. Dourandin, W.D. Huang, N.P. Luneva, N.E. Geacintov, J. Phys. Chem. B 103 (1999) 10924.
[14] Y. Hirata, N. Mataga, Y. Sakata, S. Misumi, J. Phys. Chem. 90 (1986) 6065.
[15] J.T. Richards, G. West, J.K. Thomas, J. Phys. Chem. 74 (1970) 4137.
[16] M. Sato, T. Kaieda, K. Ohmukai, H. Kawazumi, T. Ogawa, Anal. Sci. 14 (1998) 855.
[17] C.L. Braun, T.W. Scott, J. Phys. Chem. 87 (1983) 4776.
[18] K. Nakashima, M. Kise, T. Ogawa, H. Kawazumi, S. Yamada, Chem. Phys. Lett. 231 (1994) 81.
[19] C.L. Braun, T.W. Scott, J. Phys. Chem. 91 (1987) 4436.
[20] Y. Mori, A. Yoneda, H. Shinoda, T. Kitagawa, Chem. Phys. Lett. 183 (1991) 584.
[21] A. Kellmann, F. Tfibel, Chem. Phys. Lett. 69 (1980) 61.
[22] L.J. Johnston, N.P. Schepp, J. Am. Chem. Soc. 115 (1993) 6564.
[23] S. Yamada, A. Hino, K. Kano, T. Ogawa, Anal. Chem. 55 (1983) 1914.
[24] Y. Taniguch, Y. Nishina, N. Mataga, Bull. Chem. Soc. Jpn. 45 (1972) 2923.
[25] S.S. Shukla, J.F. Rusling, J. Phys. Chem. 89 (1985) 3353.
[26] H.J. Shine, D.C. Zhao, J. Org. Chem. 55 (1990) 4086.

[27] D.T. Breslin, M.A. Fox, J. Phys. Chem. 98 (1994) 408.
[28] T. Nakabayashi, S. Kamo, H. Sakuragi, N. Nishi, J. Phys. Chem. A 105 (2001) 8605.
[29] D. Molho, J. Coillard, Bull. Soc. Chim. France (1956) 78.
[30] J.I.G. Cadogan, E.G. Duell, P.W. Inward, J. Chem. Soc. (1962) 4164.
[31] R.F.B. Cox, J. Am. Chem. Soc. 62 (1940) 3512.
[32] M. Oki, Y. Urushibara, Bull. Chem. Soc. Jpn. 25 (1952) 109.
[33] E. Maccarone, A. Mamo, G. Perrini, M. Torre, J. Chem. Soc., Perkin Trans. 2 (1981) 324.
[34] L. Zechmeister, W.H. McNeely, J. Am. Chem. Soc. 64 (1942) 1919.
[35] U. Mazzucato, Pure Appl. Chem. 54 (1982) 1705.
[36] N.J. Turro, Modern Molecular Photochemistry, University Science Book, Sausalito, 1991.
[37] F.D. Lewis, X.Y. Liu, S.E. Miller, R.T. Hayes, M.R. Wasielewski, J. Am. Chem. Soc. 124 (2002) 11280.
[38] L. Nikowa, D. Schwarzer, J. Troe, J. Schroeder, J. Chem. Phys. 97 (1992) 4827.
[39] W. Rettig, Angew. Chem. Int. Ed. Engl. 25 (1986) 971.
[40] Y.V. IlIchev, W. Kuhnle, K.A. Zachariasse, Chem. Phys. 211 (1996) 441.
[41] M.O. Delcourt, M.J. Rossi, J. Phys. Chem. 86 (1982) 3233.
[42] I.P. Bell, M.A.J. Rodgers, H.D. Burrows, J. Chem. Soc., Faraday Trans l 73 (1977) 315.
[43] T. Majima, M. Fukui, A. Ishida, S. Takamuku, J. Phys. Chem. 100 (1996) 8913.
[44] F.D. Lewis, A.M. Bedell, R.E. Dykstra, J.E. Elbert, I.R. Gould, S. Farid, J. Am. Chem. Soc. 112 (1990) 8055.
[45] F.D. Lewis, R.E. Dykstra, I.R. Gould, S. Farid, J. Phys. Chem. 92 (1988) 7042.
[46] I.R. Gould, D. Ege, J.E. Moser, S. Farid, J. Am. Chem. Soc. 112 (1990) 4290.
[47] B.H. Cumpston, S.P. Ananthavel, S. Barlow, D.L. Dyer, J.E. Ehrlich, L.L. Erskine, A.A. Heikal, S.M. Kuebler, I.Y.S. Lee, D. McCord-Maughon, J.Q. Qin, H. Rockel, M. Rumi, X.L. Wu, S.R. Marder, J.W. Perry, Nature 398 (1999) 51.
[48] M. Albota, D. Beljonne, J.L. Bredas, J.E. Ehrlich, J.Y. Fu, A.A. Heikal, S.E. Hess, T. Kogej, M.D. Levin, S.R. Marder, D. McCord-Maughon, J.W. Perry, H. Rockel, M. Rumi, C. Subramaniam, W.W. Webb, X.L. Wu, C. Xu, Science 281 (1998) 1653.